# Isotope Shift Calculations

# Quantum Chemical Calculations of Vibrational Frequencies and Associated Isotope Shifts in $SF_6$, $MoF_6$, and $UF_6$: A DFT Study

**Ayan Ghosh* and J. Padma Nilaya**

*Laser and Plasma Technology Division, Beam Technology Development Group,*
*Bhabha Atomic Research Centre, Mumbai-400085, India*

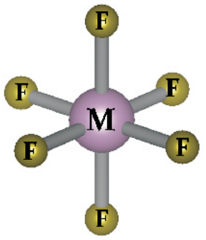

Structure of $MF_6$ (M = S, Mo, and U)
$O_h$ Symmetry

ABSTRACT

The accuracy of the performance of DFT functional in estimating the vibrational isotope shift in any chemical system motivated us to determine the isotope shift of the fundamental vibrational modes of $SF_6$, $MoF_6$, and $UF_6$ molecules by employing B3LYP, PBE0, and M06 functionals. They have also been employed to explore the molecular structure, stability, harmonic vibrational frequencies, and charge distribution. The isotope shifts ($\Delta\nu_3$) have been found to be 17.1-17.8, 1.0-1.2, and 0.63-0.67cm$^{-1}$ for the $^{32}SF_6$-$^{34}SF_6$, $^{97}MoF_6$-$^{98}MoF_6$, and $^{235}UF_6$-$^{238}UF_6$ isotopomers, respectively, that agree well with the experimentally measured isotope shifts.

KEYWORDS: *Hexafluorides, Density Functional Theory, Structure and Stability, Vibrational Frequency, Isotope Shift.*

## Introduction

Enrichment of relevant isotopes through efficient techniques is important for the front-end of the Indian nuclear fuel cycle and medical industry in addition to being a deterrent in the current world scenario. The enrichment of the $^{235}U$ isotope (natural abundance 0.72%) understandably therefore, assumes a significant role. Of the many radio-isotopes employed in radiopharmaceutical industry, $^{32}P$ that is used for the bone pain palliation in the skeletal metastases is produced in N-reactor through the bombardment of $^{32}S$ by fast neutrons. $^{99m}Tc$ radio-isotope is known as the 'Work Horse' in Nuclear Medicine as more than 80% of radiopharmaceuticals use this isotope. It is prepared from the $^{99}Mo/^{99m}Tc$ generator where $^{99}Mo$ itself is produced in a nuclear reactor through $^{98}Mo\ (n, \gamma)\ ^{99}Mo$ reaction. $^{99}Mo$ emits particle and eventually decays to $^{99m}Tc$. Since the medical radio-isotopes are administered to the patients, the radio-chemical as well as the radio-nuclide purity is of utmost importance. To obtain the required specific activity, $^{32}S$ and $^{98}Mo$ having natural abundances 94.99% and 24.29% need to be suitably enriched.

Among all the existing enrichment processes, *viz.*, gas diffusion, gas centrifuge, electromagnetic separator, laser isotope separation (LIS) processes, the LIS is considered most promising as it is known to be an energy efficient process with a relatively much smaller foot print. The LIS process that employs molecular gas as the working medium, termed the molecular laser isotope separation (MLIS) where the desired isotopic species is selectively excited and separated through infrared multi-photon dissociation (IRMPD) was earlier considered impractical owing to the requirement of prohibitively high power of coherent light. However, there has been a resurgence of interest in it of late due to the so called SILEX (Separation of Isotopes by Laser Excitation) technology[1] that, although not explicitly spelt out in open literature, is most likely based on low-energy processes[2]. In this direction, very recently, Makarov and co-workers have reported very high enrichment factor for $^{34}S$ isotope in $SF_6$ by employing the laser assisted gasdynamic expansion scheme[3].

Due to several advantages, *viz.*, the mono-isotopy of fluorine atom, higher vapor pressure, gaseous form at room temperature, the $MF_6$ (M = S/Mo/U) is considered to be the most suitable molecule for the separation of isotopes of S, Mo, and U. It is essential to have a prior knowledge of the vibrational frequencies and the associated isotope shifts of the molecules of interest to be able to selectively excite the desired isotopic species and separate it from the rest. This information may not be obtainable from literature for all molecules of interest and hence the calculation of the vibrational frequencies and the corresponding isotopic shifts assumes significance. In this article, we present the geometry optimization of a molecule followed by the vibrational frequency calculations for obtaining the isotope shift in $SF_6$, $MoF_6$, and $UF_6$ molecules by employing density functional theory (DFT).

## Computational Methodology

All the theoretical computations have been carried out by using density functional theory based methods in Turbomole-7.2.1 software[4]. The structures of $MF_6$ (M = S, Mo, and U) have been optimized in singlet ground electronic spin state using two hybrid DFT GGA functionals, *viz.*, Becke three-parameter exchange and Lee–Yang–Parr correlation (B3LYP)[5] and hybrid form of Perdew-Burke-Ernzerhof exchange and correlation (PBE0) [6]; and a hybrid DFT meta-GGA functional,

---

**Author for Correspondence: Ayan Ghosh*
*E-mail: ghosha@barc.gov.in*

*Table 1: Optimized M-F bond length ($R_{M-F}$) in Å), Partial NPA charges on 'M' atom ($q_M$) and each 'F' atom ($q_F$), HOMO Energy ($E_{HOMO}$) and LUMO Energy ($E_{LUMO}$) and their gaps ($\Delta E_{Gap}$) in eV for $MF_6$ (M = S, Mo, and U) molecules by using B3LYP, PBE0, and M06 methods with DEF2 basis set.*

| Molecule | Methods | $R_{M-F\ (Calc.)}$ | $R_{M-F\ (Expt.)}$ | $q_M$ | $q_F$ | $E_{HOMO}$ | $E_{LUMO}$ | $\Delta E_{Gap}$ |
|---|---|---|---|---|---|---|---|---|
| $SF_6$ | B3LYP | 1.580 | 1.561[a] | 2.612 | −0.435 | −12.025 | −2.109 | 9.917 |
| | PBE0 | 1.566 | | 2.610 | −0.435 | −12.405 | −1.295 | 11.109 |
| | M06 | 1.558 | | 2.679 | −0.446 | −12.455 | −1.349 | 11.106 |
| $MoF_6$ | B3LYP | 1.817 | 1.817[b] | 2.427 | −0.404 | −12.349 | −5.869 | 6.480 |
| | PBE0 | 1.817 | | 2.434 | −0.406 | −12.743 | −5.549 | 7.193 |
| | M06 | 1.820 | | 2.475 | −0.413 | −12.825 | −5.672 | 7.152 |
| $UF_6$ | B3LYP | 2.007 | 1.996[c] | 2.358 | −0.393 | −-11.855 | −6.460 | 5.395 |
| | PBE0 | 1.988 | | 2.335 | −0.389 | −12.120 | −6.000 | 6.120 |
| | M06 | 1.994 | | 2.412 | −0.402 | −12.249 | −6.352 | 5.897 |

[a]Ref. [10]; [b]Ref. [11]; [c]Ref. [12]

*i.e.*, Minnesota exchange-correlation-2006 hybrid with 27% HF exchange (M06) [7]. For F, S, and Mo (28 electrons ECP) atoms, we have used def2-TZVPP basis set [8] while def-TZVPP basis set[8] has been employed for the U (60 electrons ECP) atom as implemented in the Turbomole software. This combination of basis set is defined as DEF2. The accuracy of the electron density based (DFT) methods coupled with basis sets is well known for the calculation of the electronic structure of any molecular system and its properties. The choice of larger basis set (DEF2) along with the abovementioned DFT functionals has shown to yield accurate results[9] in the electronic structure calculations of any chemical system using molecular orbital theory based techniques.

### Optimized Structural Parameters of $MF_6$

The DFT based methods with B3LYP, PBE0, and M06 functionals have been employed to optimize the electronic structures of all the $MF_6$ (M =S, Mo, and U) molecules and the true minima in their respective singlet potential energy surfaces is obtained. The optimized structure of $MF_6$ (Fig.1) exhibits octahedral geometry having $O_h$ symmetry at its minima. Table 1 lists the M-F bond distances in all the $MF_6$ (M = S, Mo, and U) molecules as obtained by using all the three abovementioned methods. The M-F bond lengths have been found to be in the range of 1.558-1.580, 1.817-1.820, and 1.988-2.007Å in $SF_6$, $MoF_6$, and $UF_6$ molecules, respectively, and the corresponding experimental values are 1.561, 1.817, 1.996Å. From the above results, it is evident that the calculated M-F bond distances are in close proximity with the experimental data lending credence to the adopted methodology.

### Stabilities of $MF_6$ Molecules

The stability of any molecular system can be inferred from their HOMO-LUMO energy gaps (Energy gap between the highest occupied molecular orbital and lowest unoccupied molecular orbital) and the same for $MF_6$ molecules have been reported in Table 1 as obtained by employing all the adopted methods. Here, the S, Mo, and U atoms are bonded with the highest electronegative element F atom whereby the HOMO is stabilized significantly for all the $MF_6$ molecules. The computed values of HOMO-LUMO gap are in the range of 9.917-11.109, 6.480-7.193, and 5.395-6.120eV for $SF_6$, $MoF_6$, and $UF_6$, respectively. Higher value of $\Delta E_{Gap}$ for all the $MF_6$ systems studied here clearly emphasizes the greater stability of the systems with a very strong M–F bond.

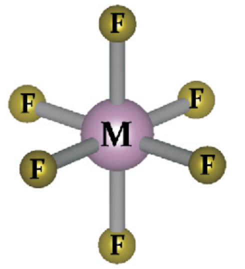

*Fig.1: Optimized structure ($O_h$) of $MF_6$ (M=S, Mo, U).*

### Natural Population Analysis (NPA) of $MF_6$

The computed net NPA charges on M and F atoms in $MF_6$ (M = S, Mo, and U) have been reported in Table 1 as obtained by all the DFT functionals. From the Table 1, it is clearly evident that there is a significant charge distribution among all the constituent atoms in all the $MF_6$ molecules. The charges acquired by the M atoms are found to be 2.612, 2.427, 2.358 along the series S–Mo–U, while the corresponding charge residing on each F atom are -0.435, -0.404, -0.393 in $SF_6$, $MoF_6$, and $UF_6$ molecules, respectively, as obtained by B3LYP

*Table 2: Fundamental vibrational frequencies ($\nu_i$ in $cm^{-1}$) for $^{32}SF_6$ along with the isotope shift ($\Delta\nu_i$ in $cm^{-1}$) for the $^{34}SF_6$ isotopomer in the parenthesis.*

| Modes (Deg.) | B3LYP | PBE0 | M06 | Expt.[a] |
|---|---|---|---|---|
| $\nu_1$ ($A_{1g}$) | 743.3 | 777.9 | 801.5 | 774.5 |
| $\nu_2$ ($E_g$) | 616.1 | 645.1 | 655.9 | 643.4 |
| $\nu_3$ ($T_{1u}$) | 909.7<br>(17.1) | 956.1<br>(17.8) | 976.9<br>(17.4) | 947.9<br>(17.1) |
| $\nu_4$ ($T_{1u}$) | 590.3<br>(2.7) | 607.2<br>(2.9) | 632.4<br>(2.8) | 615.0<br>(2.6) |
| $\nu_5$ ($T_{2g}$) | 502.5 | 516.0 | 537.0 | 523.5 |
| $\nu_6$ ($T_{2u}$) | 329.5 | 341.1 | 363.2 | 346.9 |

[a]Ref. [10]

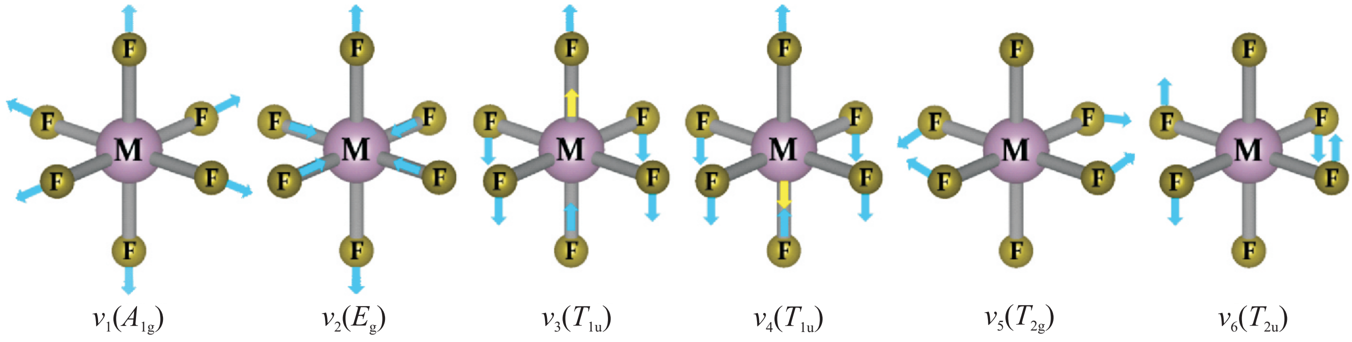

*Fig.2: Fundamental vibrational modes of the hexafluoride ($MF_6$, M = S, Mo, and U) molecules.*

method with DEF2 basis set. This implies that the positive (~+2) charge residing on the M center is being neutralized by the six negatively charged F atoms via electron transfer from the M atoms to the F atoms. This is attributed to the strong covalent M–F bond with large charge delocalization and electrostatic interaction between the oppositely charged centers.

### Vibrational Frequency Analysis and Estimation of Isotope Shift in $MF_6$

One of the best ways to test the accuracy of any method is to analyze its ability to reproduce the vibrational frequencies of the molecular system. We have performed harmonic vibrational analysis in order to distinguish the different vibrational modes for the characterization of the $MF_6$ chemical system. In this context, it is to be noted that two electron density based methods (B3LYP and M06 functionals) accurately compute the vibrational frequency for the DHP ($^{12}C_5H_8{}^{16}O$) molecule, as can be seen when matched with the experimentally available data for abundant isotope[9]. Among various DFT functionals, B3LYP, PBE0, and M06 have been found to reproduce the vibrational frequency more accurately for all the hexafluoride ($MF_6$, M = S, Mo, and U) molecules. Therefore, the calculated vibrational frequency values for the $SF_6$, $MoF_6$, and $UF_6$ molecules at B3LYP/DEF2, PBE0/DEF2, and M06/DEF2 levels are given in Table 2, 3 and 4, respectively.

Since the octahedral ($O_h$) geometry is the lowest energy structure of all the $MF_6$ molecules, therefore, all the molecules possess six fundamental modes of vibrations, *viz.*, $\nu_1$-$\nu_6$. Among all the modes, $\nu_1$ is non-degenerate ($A_{1g}$), $\nu_2$ is doubly degenerate ($E_g$), and $\nu_3$-$\nu_6$ are triply degenerate ($T_{1u}$, $T_{1u}$, $T_{2g}$, $T_{2u}$) vibrational modes. Being a centrosymmetric molecule, Raman active modes cannot be IR active and vice-versa. Therefore, $MF_6$ has three Raman-active ($\nu_1$, $\nu_2$, $\nu_5$) modes, two IR-active ($\nu_3$, $\nu_4$) modes, and one forbidden ($\nu_6$) mode. Tables 2, 3, and 4 include all possible vibrational frequencies computed using the aforementioned DFT functionals, along with their degeneracy for the $MF_6$ molecules.

*Table 3: Fundamental vibrational frequencies ($\nu_i$ in $cm^{-1}$) for $^{98}MoF_6$ along with the isotope shift ($\Delta\nu_i$ in $cm^{-1}$) for the $^{97}MoF_6$ isotopomer in theparenthesis.*

| Modes (Deg.) | B3LYP | PBE0 | M06 | Expt.[a] |
|---|---|---|---|---|
| $\nu_1$ ($A_{1g}$) | 739.2 | 762.2 | 751.8 | 741.0 |
| $\nu_2$ ($E_g$) | 642.8 | 661.1 | 654.2 | 643.0 |
| $\nu_3$ ($T_{1u}$) | 732.6<br>(1.0) | 750.4<br>(1.1) | 737.8<br>(1.2) | 741.0<br>(1.0) |
| $\nu_4$ ($T_{1u}$) | 257.2<br>(0.3) | 259.0<br>(0.4) | 264.3<br>(0.4) | 264.0<br>(0.2) |
| $\nu_5$ ($T_{2g}$) | 307.6 | 311.3 | 309.8 | 306.0 |
| $\nu_6$ ($T_{2u}$) | 118.9 | 120.6 | 135.7 | 190.0 |

[a]Ref. [11]

*Table 4: Fundamental vibrational frequencies ($\nu_i$ in $cm^{-1}$) for $^{238}UF_6$ along with the isotope shift ($\Delta\nu_i$ in $cm^{-1}$) for the $^{235}UF_6$ isotopomer in the parenthesis.*

| Modes (Deg.) | B3LYP | PBE0 | M06 | Expt.[a] |
|---|---|---|---|---|
| $\nu_1$ ($A_{1g}$) | 662.0 | 684.9 | 663.3 | 663.9 |
| $\nu_2$ ($E_g$) | 532.7 | 543.5 | 514.8 | 529.8 |
| $\nu_3$ ($T_{1u}$) | 617.2<br>(0.63) | 635.6<br>(0.63) | 614.1<br>(0.67) | 627.5<br>(0.65) |
| $\nu_4$ ($T_{1u}$) | 188.4<br>(0.2) | 189.8<br>(0.2) | 182.8<br>(0.3) | 189.1<br>(0.2) |
| $\nu_5$ ($T_{2g}$) | 200.9 | 201.5 | 187.9 | 193.7 |
| $\nu_6$ ($T_{2u}$) | 143.2 | 145.2 | 147.7 | 147.6 |

[a]Ref. [12]

The pictorial representation of all the vibrational modes as obtained computationally agrees very well with experimental findings is represented in Fig.2. Since irradiation of the $MF_6$ molecules is possible with IR lasers, $\nu_3$ and $\nu_4$ modes are of our interest. Between $\nu_3$ and $\nu_4$, the frequency value for the $\nu_3$ mode is higher than the corresponding $\nu_4$ mode and generally, the isotope selective excitation of the $\nu_3$ vibrational mode has been attempted experimentally. For the highest abundant isotopes, the calculated vibrational frequencies for $\nu_3$ mode in $^{32}SF_6$, $^{98}MoF_6$, and $^{238}UF_6$ as shown in Tables 2, 3 and 4 are close to the experimental data available.

For the determination of the isotope shift ($\Delta\nu$), the IR frequencies have been calculated for all the isotopomers of $MF_6$. The difference in vibrational frequency with respect to that of the molecule with abundant isotopic species is termed 'Isotope Shift'. For $SF_6$, the isotope shift ($\Delta\nu_3$) values have been found to be 8.5-8.9 and 17.1-17.8$cm^{-1}$ for the $^{32}SF_6$-$^{33}SF_6$ and $^{32}SF_6$-$^{34}SF_6$ isotopomers, respectively, while the corresponding experimental values are 8.6 and 17.1 $cm^{-1}$. In case of $MoF_6$, 1.0-1.2 and 2.1-2.4$cm^{-1}$ are the isotope shifts between the $^{97}MoF_6$-$^{98}MoF_6$ and $^{98}MoF_6$-$^{100}MoF_6$ pairs. The isotope shift value was found to be 0.63-0.67$cm^{-1}$ for $^{235}UF_6$ and $^{238}UF_6$ isotopomer while the experimentally measured value from literature is

0.65 $cm^{-1}$. As can be seen, the calculated values match pretty well with the experimental data available. The slight variation in the theoretically computed fundamental vibrational frequency values with the experimental data may also arise due to the anharmonicity effect which should be considered for precise determination of isotope shift. Further, the harmonic vibrational frequency analysis through some DFT functionals (B3LYP, PBE0, and M06) seem more promising methods for accurate determination of the isotope shift as reported by us[9].

## Conclusion

The first principle based density functional theory based methods are important theoretical tools for the calculations of isotope shifts in the fundamental vibrational modes of the isotopomers. In order to determine the isotope shift, the geometry of the $MF_6$ (M = S, Mo, and U) molecules has been first optimized followed by fundamental vibrational frequency calculation for the different isotopomers of the molecules of interest. Knowledge of the fundamental vibrational frequencies and the corresponding isotope shifts play an important role in the choice of the process gas, the laser to be employed and the process parameter in molecular based laser isotope separation process.

## Acknowledgements

The authors thank the Computer Division, Bhabha Atomic Research Centre for providing computational facilities and express gratitude to Tapan K. Ghanty, M. Mascarenhas, and Archana Sharma for their kind interest and encouragement.

## References

[1] (a) www.silex.com.au; (b) SILEX Process www.chemeurope.com/en/encyclopedia/Silex_Process.html; (c) SILEX Uranium Enrichment SILEX Annual Report (2014), www.silex.com.au; (d) SILEX Uranium Enrichment SILEX Annual Report (2017), www.silex.com.au.

[2] J. L. Lyman, Enrichment separative capacity for SILEX Report LA-UR-05-3786 (2005) Los Alamos National Laboratory.

[3] V. N. Lokhman, G. N. Makarov, A. L. Malinovskii, A. N. Petin1, D. G. Poydashev, and E. A. Ryabov, Isotope-Selective Control of the Clusterization of $SF_6$ Molecules by an IR Laser during Gasdynamic Expansion of an $SF_6$/Ar Mixture. *Laser Phys.*, 2018, **28**, 105703, https://doi.org/10.1088/1555-6611/aad289.

[4] R. Ahlrichs, M. Bär, M. Häser, H. Horn, and C. Kölmel, Chem. Phys. Lett., 1989, **162**, 165. Available from http://www.turbomole.com.

[5] (a) A. D. Becke, A New Mixing of Hartree-Fock and Local Density-Functional Theories. J. Chem. Phys., 1993, **98**, 1372-1377, https://doi.org/10.1063/1.464304; (b) C. Lee, W. Yang, and R. G. Parr, Development of the Colle-Salvetti Correlation-Energy Formula into a Functional of the Electron Density. Phys. Rev. B, 1988, **37**, 785-789, https://doi.org/10.1103/PhysRevB.37.785.

[6] M. Ernzerhof and G. Scuseria, Assessment of the Perdew. Burke. Ernzerhof Exchange-Correlation Functional. J. Chem. Phys., 1999, **110**, 5029. https://doi.org/10.1063/1.478401.

[7] Y. Zhao and D. G. Truhlar, The M06 Suite of density functionals for Main Group Thermochemistry, Thermochemical Kinetics, Noncovalent Interactions, Excited States, and Transition Elements: Two New Functionals and Systematic Testing of Four M06-Class Functionals and 12 Other Functional. Theoret. Chem. Acc., 2008, **120**, 215-241, https://doi.org/10.1007/s00214-007-0310-x; Err. Theoret. Chem. Acc., 2008, **119**, 525. https://doi.org/10.1007/s00214-007-0401-8.

[8] F. Weigend and R. Ahlrichs, Balanced Basis Sets of Split Valence, Triple Zeta Valence and Quadruple Zeta Valence Quality for H to Rn: Design and Assessment of Accuracy. Phys. Chem. Chem. Phys., 2005, **7**, 3297-3305. https://doi.org/10.1039/B508541A

[9] A. Ghosh and J. P. Nilaya, Ab initio and DFT Benchmark Study for the Calculations of Isotopic Shifts of Fundamental Frequencies for 2,3-Dihydropyran. Struct. Chem., 2022. https://doi.org/10.1007/s11224-021-01829-4.

[10] R. S. McDowell, B. J. Krohn, H. Flicker, and M. C. Vasquez, Vibrational levels and anharmonicity in $SF_6$- I. Vibrational band analysis. Spectrochim. Acta., 1986, **42A**, 351- 369. https://doi.org/10.1016/0584-8539(86)80199-4.

[11] H. H. Claassen, H. Selig, and J. G. Malm, Vibrational Spectra of $MoF_6$ and $TcF_6$. J. Chem. Phys., 1962, **36**, 2888- 2890. https://doi.org/10.1063/1.1732396.

[12] D. M. Cox, and J. Elliott, IR Spectroscopy of $UF_6$, Spectrosc. Lett., 1979, **12**, 275-280. https://doi.org/10.1080/00387017908069153.